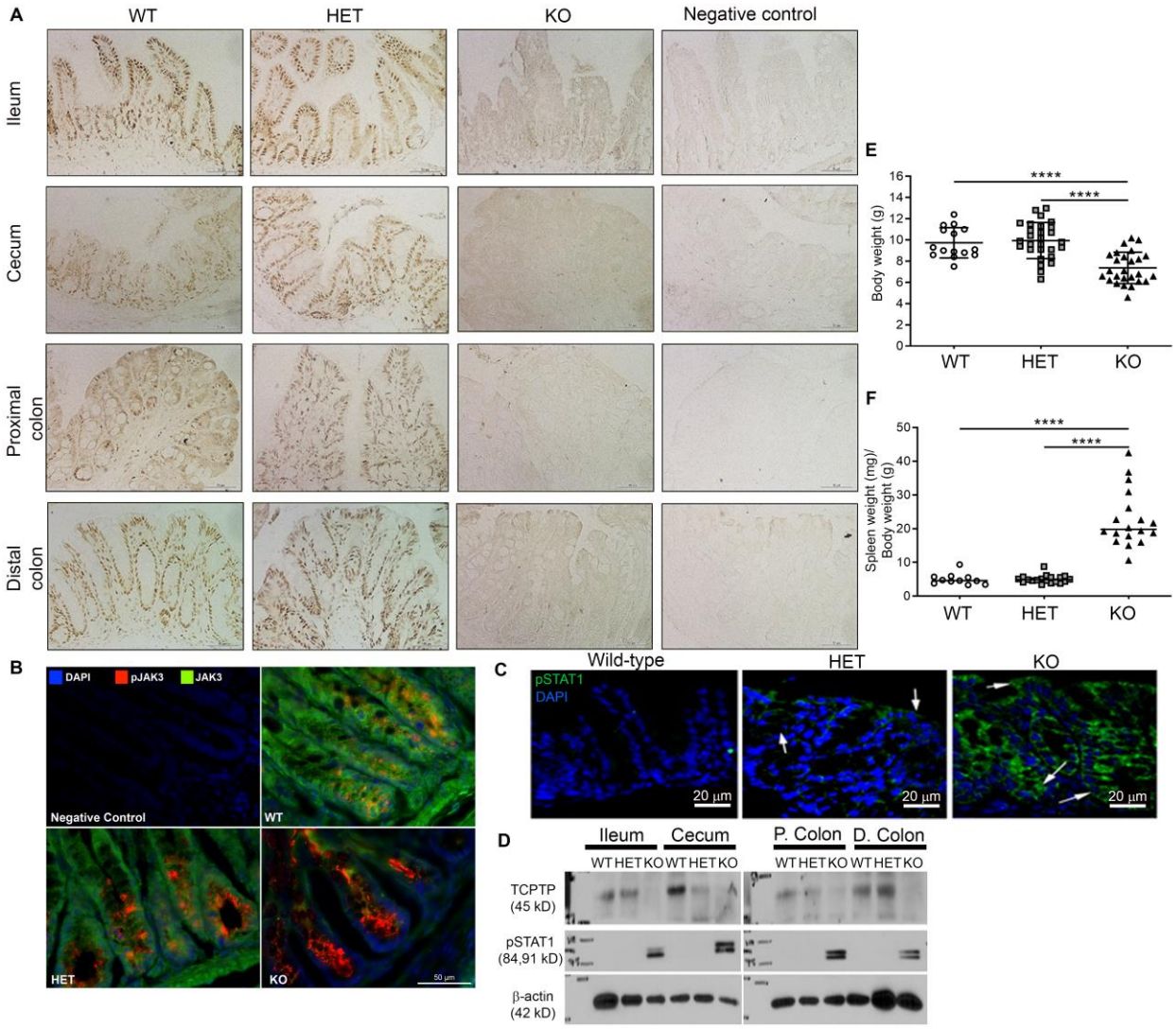


**Supplementary Figure 1. *Tcptp*-deficient mice exhibit elevated intestinal epithelial JAK-STAT activation.** (**A**) Representative immunostaining of TCPTP expression in ileum, cecum, proximal and distal colon from *Tcptp* WT, HET and KO mice. (**B**) Phosphorylation of JAK3 and expression of total JAK3 were determined in proximal colon by immunofluorescence. White arrows indicate pJAK3 signal. (**C**) Phosphorylation of the TCPTP substrate, STAT1 was determined by immunofluorescence of whole proximal colon, and (**D**) Western blotting of isolated IECs from proximal colon of WT, HET and KO mice. (n=5-7 per genotype). (**E**) Mouse body weights (grams (g)), and (**F**) spleen weight relative to body weight (mg/g) were measured.

Data are expressed as mean ± SD. Statistical significance was calculated by 1-way ANOVA and Student-Newman-Keuls post-test. ****,P<0.0001.

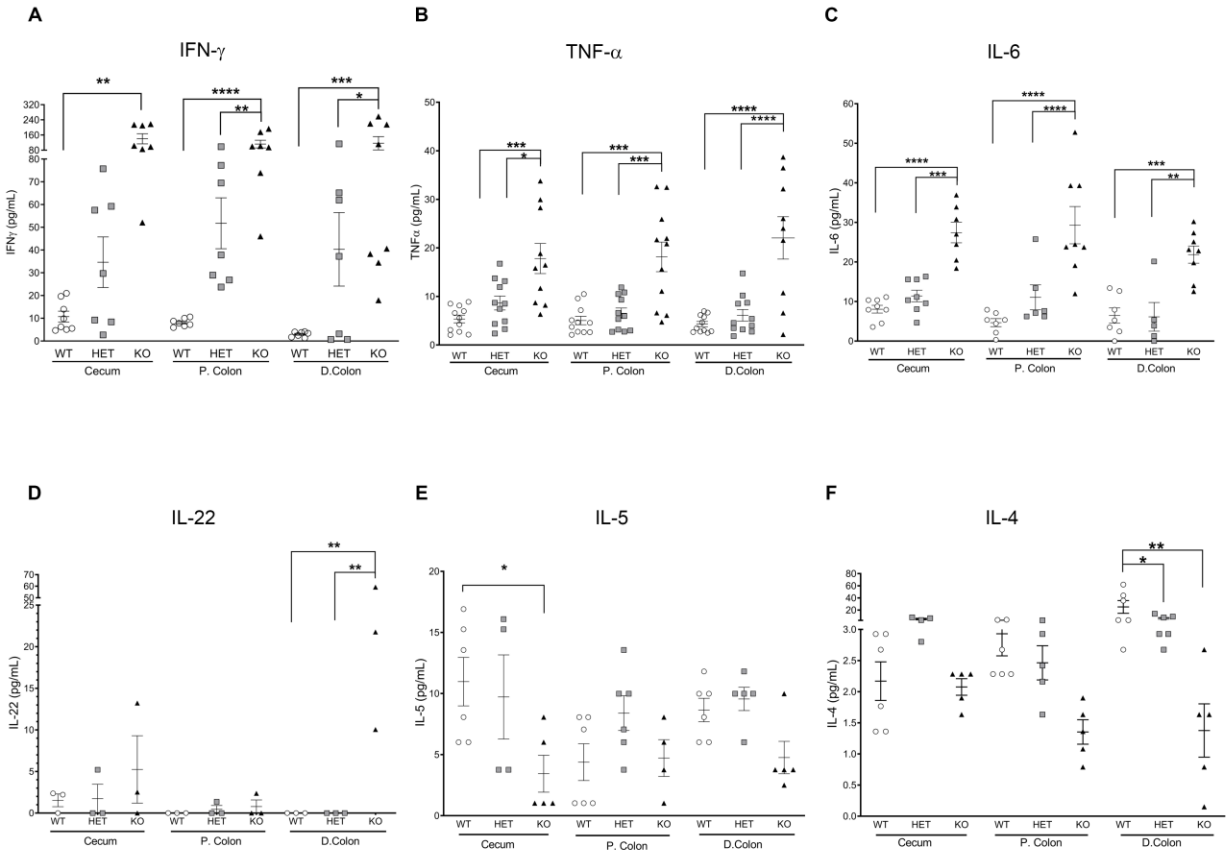


**Supplementary Figure 2. *Tcptp*-deficient mice exhibit regional variation in intestinal levels of inflammatory cytokines.** Protein levels of the cytokines (**A**) IFN-γ, (**B**) TNFα, (**C**) IL-6, (**D**) IL-22, (**E**) IL-5, and (**F**) IL-4 were quantified by Luminex Multiplex Array of whole tissue lysates from cecum, proximal colon (*P. Colon*) and distal colon (*D. Colon*) regions from 18-21 day old *Tcptp*-WT, HET or KO mice as indicated. Data are expressed as mean ± SD. In all panels, n = 3–11 mice per genotype. Statistical significance was calculated by 1-way ANOVA and Student-Newman-Keuls post-test. *P<0.05; **,P<0.01; ***,P<0.001; and ****,P<0.0001.

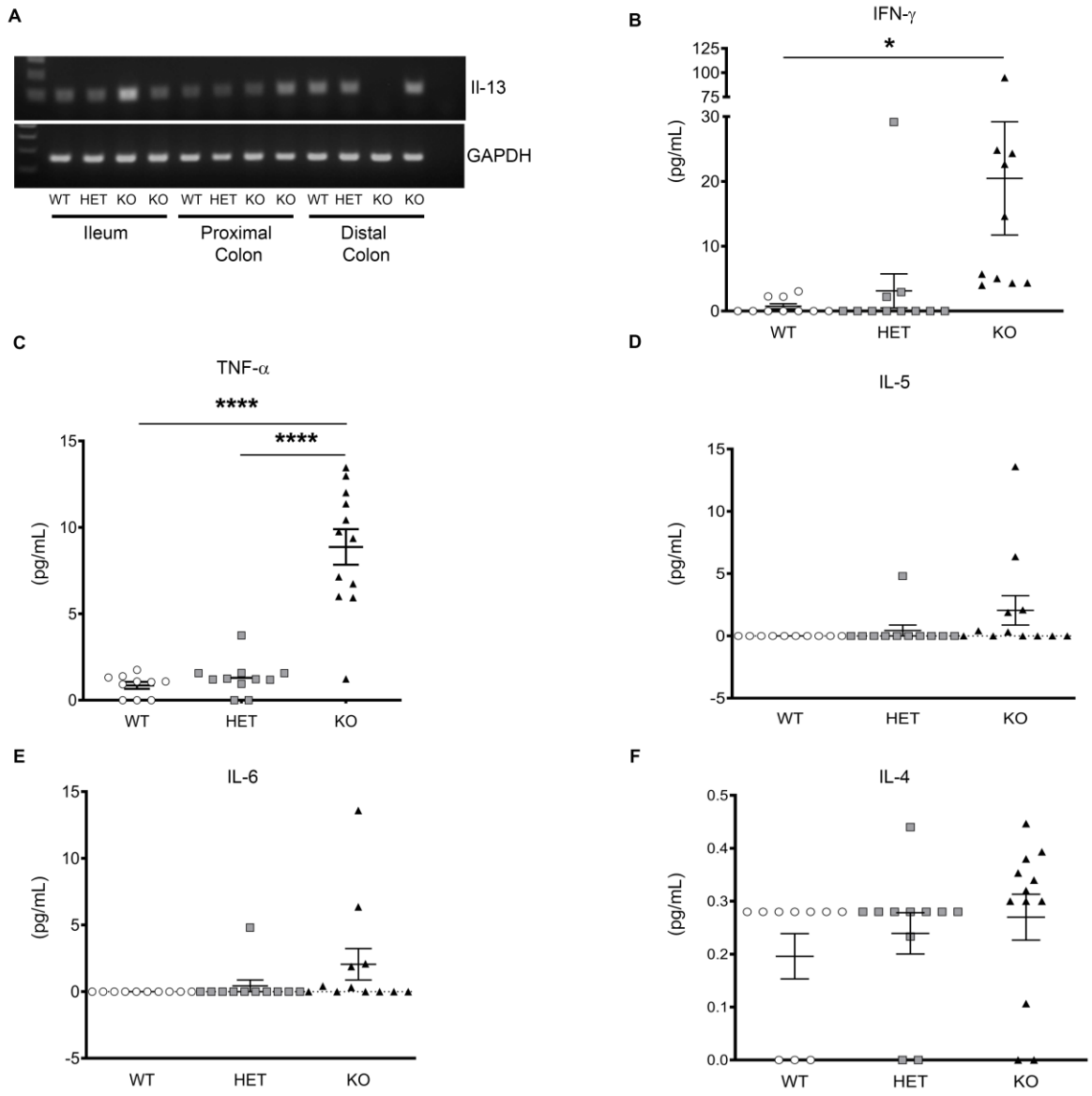


**Supplementary Figure 3. Intestinal IL-13 mRNA and serum cytokine levels in *Tcptp*-deficient mice.** (**A**) IL-13 mRNA levels in ileum, proximal colon and distal colon were determined by PCR (n=3-6). Quantification of serum levels of (**B**) IFN-γ, (**C**) TNF-α, (**D**) IL-6, (**E**) IL-5 and (**F**) IL-4 cytokines by Luminex multiplex assay (n=7-11). Data are expressed as mean ± SD. Statistical significance was calculated by 1-way ANOVA and Student-Newman-Keuls post-test. *,P<0.05; **,P<0.01; and ****,P<0.0001.

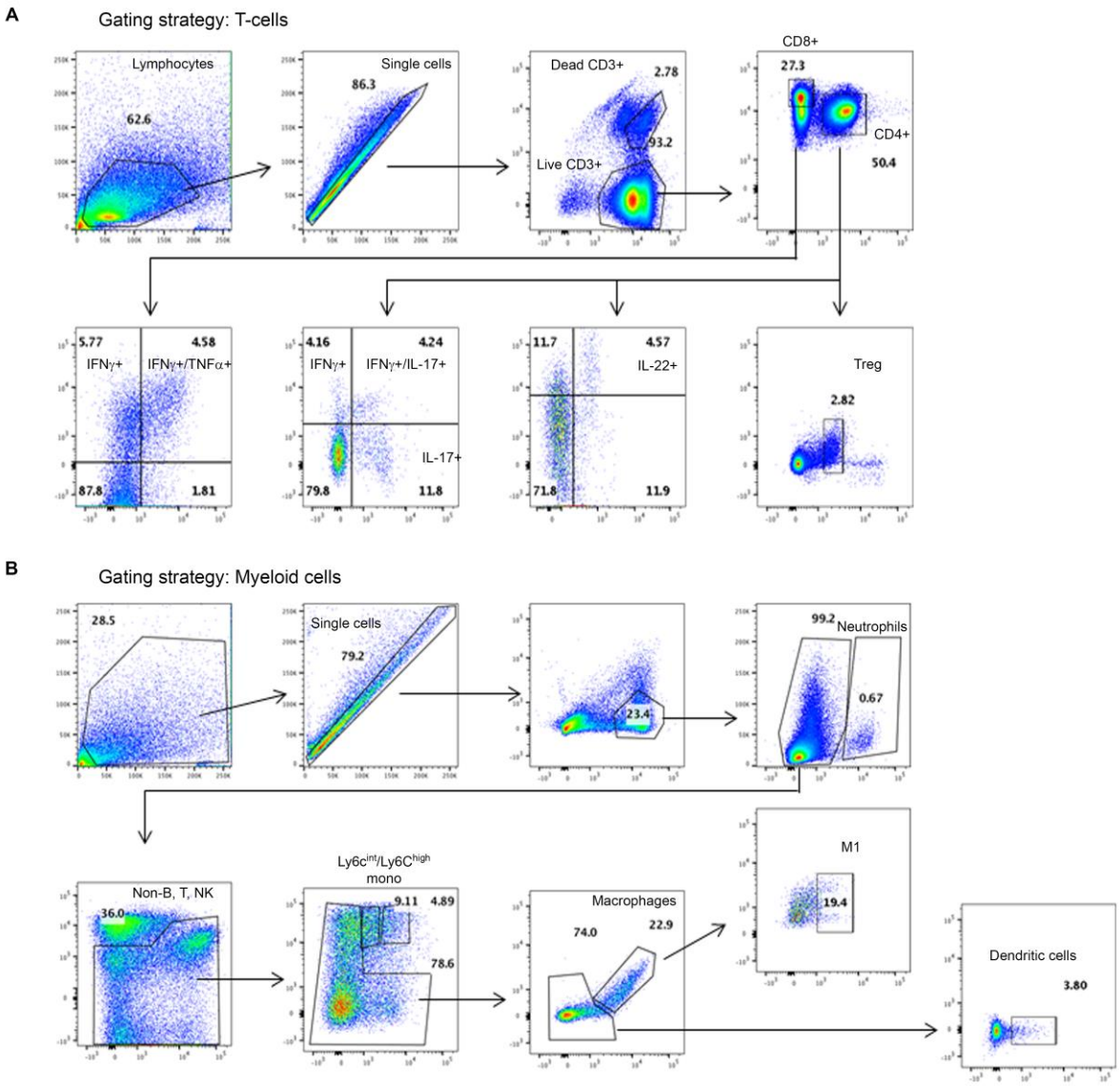


**Supplementary Figure 4. Flow cytometry gating strategy for *Ptpn2*-deficient mouse tissue immune cell characterization.** Depicted are representative flow cytometry dot plots showing the gating strategy for characterization of (**A**) T-lymphocyte and (**B**) myeloid immune cell populations, and analysis of the proportion of $CD11c^{+}MHCII^{+}$ dendritic cells and $Foxp3^{+}$ $CD4^{+}$ T cells.

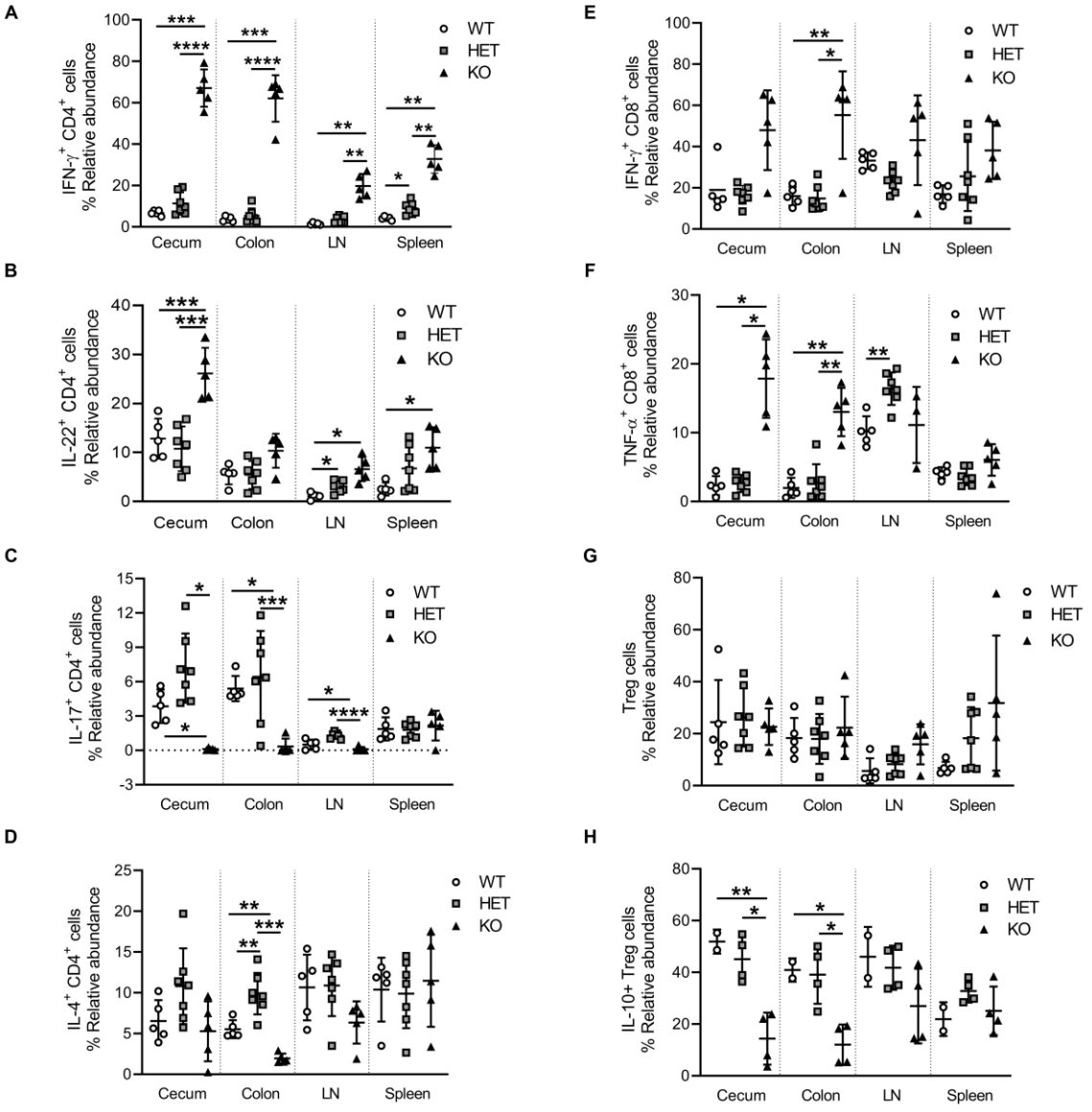


**Supplementary Figure 5. Characterization of tissue T-cell populations and cytokine expression in *Ptpn2*-deficient mice by flow cytometry.** Immune cells were isolated from the cecum and colon lamina propria, the mesenteric lymph nodes and the spleen of WT, HET and KO mice and analyzed for the proportion of (**A**) IFN$\gamma^+$ (**B**) IL-22$^+$, (**C**) IL-17$^+$, (**D**) IL-4$^+$ CD4$^+$ T cells, (**E**) IFN$\gamma^+$, and (**F**) TNF$\alpha^+$ CD8$^+$ T cells, (**G**) FoxP3$^+$ cells among CD4$^+$ T cells, and (**H**) IL-10$^+$ cells among FoxP3$^+$ CD4$^+$ T cells. Data are expressed as mean ± SD. In all panels, n = 2–6

mice per genotype. Statistical significance was calculated by 1-way ANOVA and Student-Newman-Keuls post-test. *P<0.05; **,P<0.01; ***,P<0.001, and ****,P<0.0001.

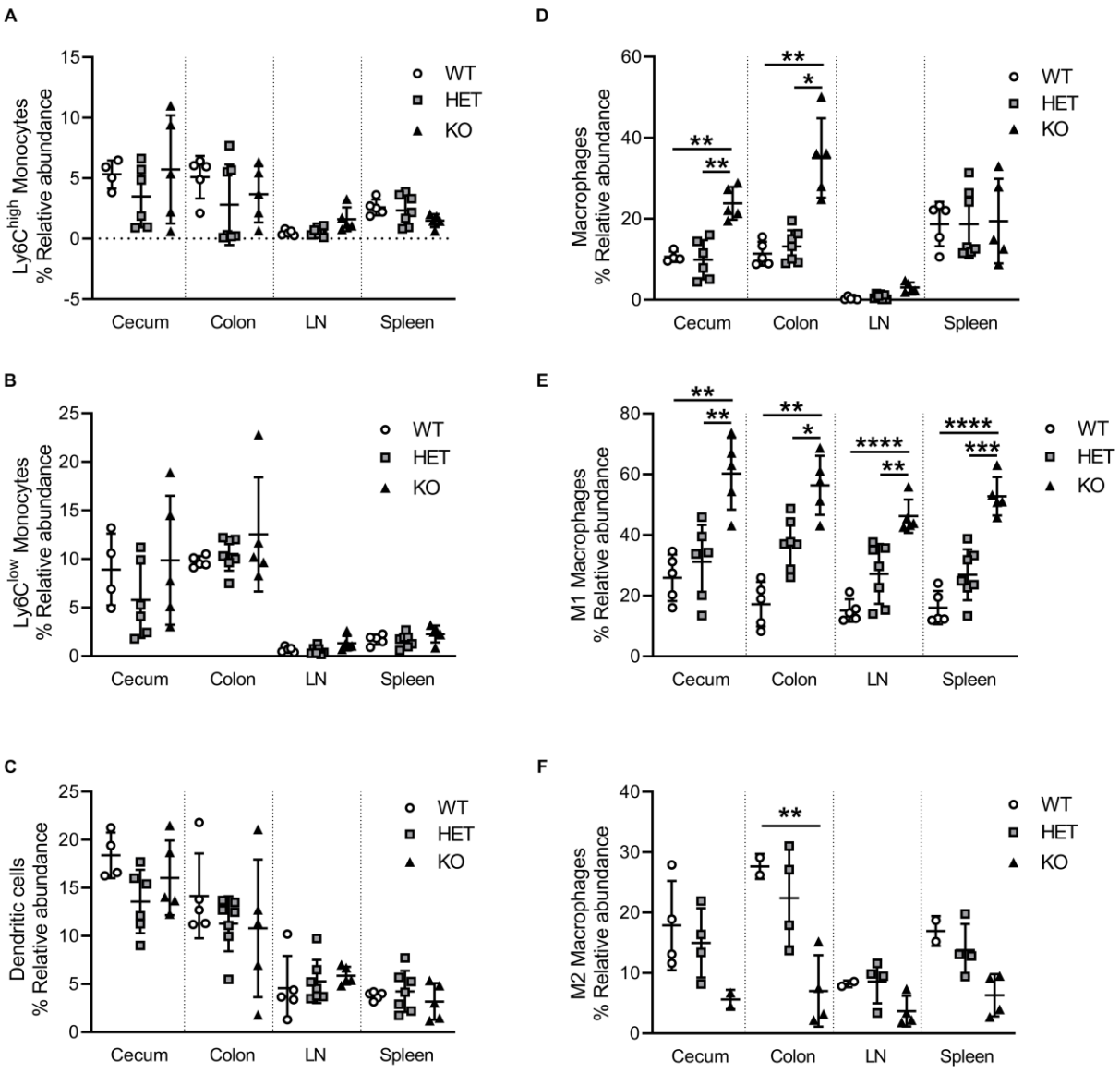


**Supplementary Figure 6. Characterization of tissue myeloid immune cells in *Ptpn2*-deficient mice by flow cytometry.** Immune cells were isolated from the cecum and colon lamina propria, the mesenteric lymph nodes and the spleen of WT, HET and KO mice and analyzed for the proportion of (**A**) Ly6Chigh and (**B**) Ly6Clow monocytes, (**C**) $CD11c^+$ $MHCII^+$ cells (dendritic cells), (**D**) $F4/80^+$ $CD64^+$ cells (macrophages), (**E**) MHCII high and (**F**) CD206 high macrophages. Data are expressed as mean ± SD. In all panels, n = 2–7 mice per

genotype. Statistical significance was calculated by 1-way ANOVA and Student-Newman-Keuls post-test. *P<0.05; **,P<0.01; ***,P<0.001; and ****,P<0.0001.

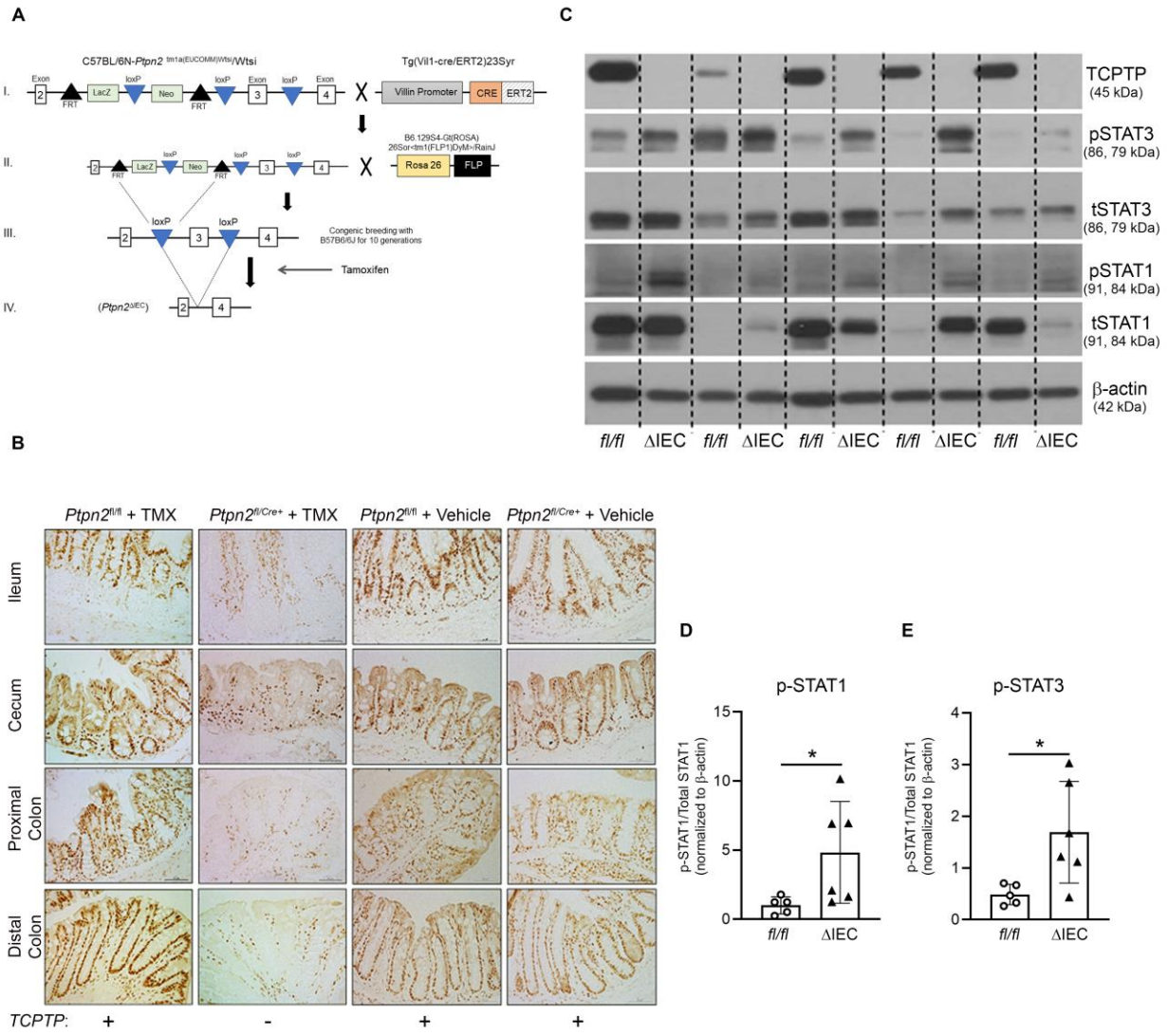


**Supplementary Figure 7. Deletion of intestinal epithelial TCPTP in *Ptpn2*$^{\Delta IEC}$knockout mice.** (**A**) Schematic of *Ptpn2*$^{\Delta IEC}$ mouse generation. (**B**) Immunohistochemistry staining for TCPTP in ileum, cecum, proximal and distal colon, shows deletion of epithelial TCPTP expression in *Ptpn2*$^{fl/Cre+}$ treated with tamoxifen (TMX) for five days and after a 28 day period to allow clearance of circulating estrogens (*Ptpn2*$^{\Delta IEC}$). IEC staining of TCPTP was unaffected in *Ptpn2*$^{\Delta IEC}$ treated with vehicle and floxed mice (*Ptpn2*$^{fl/fl}$) treated with TMX or vehicle. (**C**) Western blots of epithelial cells isolated from ileum of *Ptpn2*$^{\Delta IEC}$ (ΔIEC) and *Ptpn2*$^{fl/fl}$ (*fl/fl*) mice to detect TCPTP, total STAT1, STAT3 and β-actin levels, as well as phosphorylation of STAT1$^{(Y701)}$

and STAT3$^{(Y705)}$. (**D**) Densitometric analysis of STAT1 phosphorylation relative to total STAT1 and (**E**) STAT3 phosphorylation relative to total STAT3. Total STAT1 and STAT3 normalized to β-actin levels (n=5-6). Data are expressed as mean ± SD. Statistical significance calculated by Student's t-test. *P<0.05.

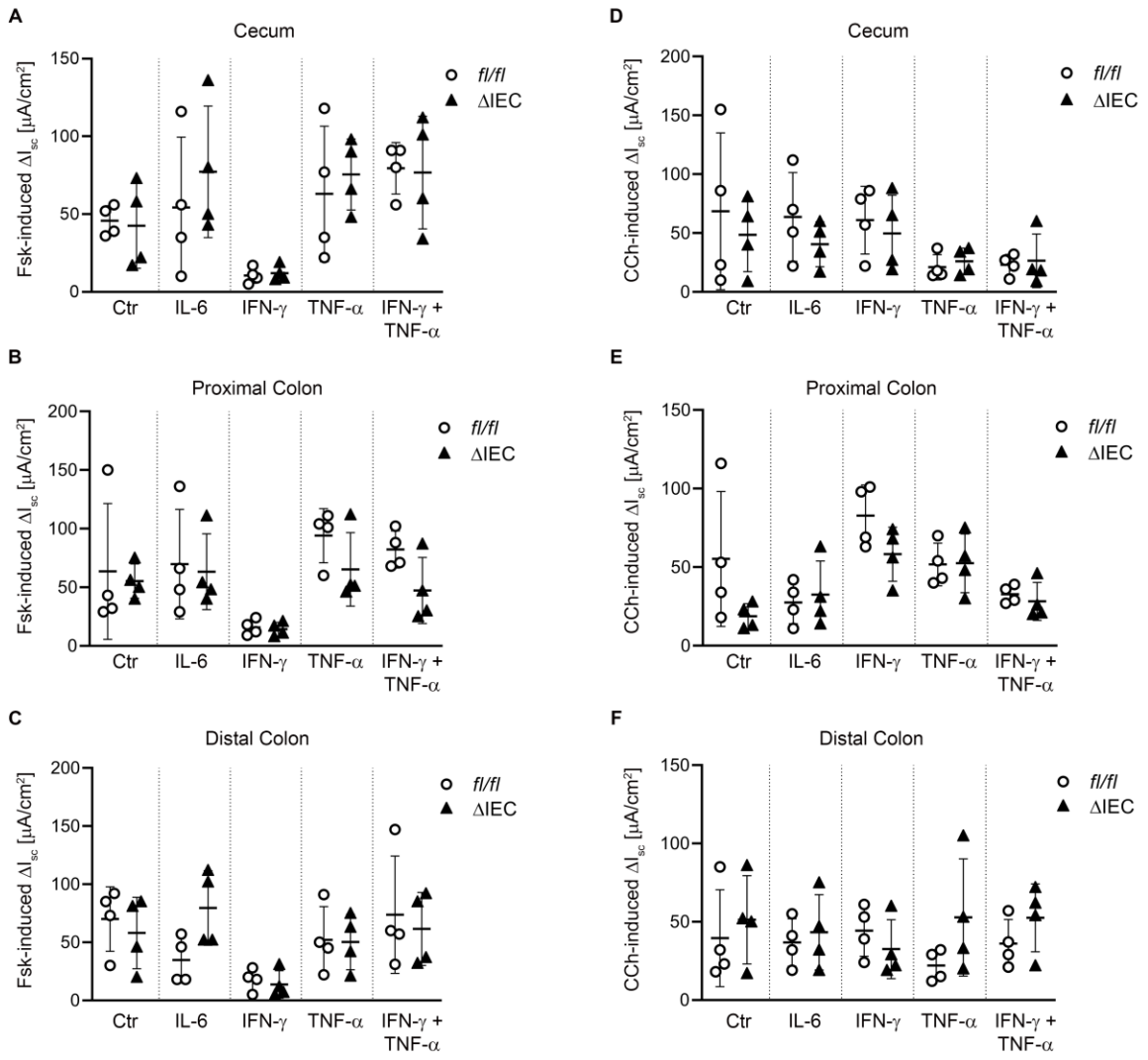


**Supplementary Figure 8. cAMP- and $Ca^{2+}$-stimulated ion transport responses of intestinal tissues from cytokine-treated *Ptpn2*$^{\Delta IEC}$knockout mice.** Following *ex vivo* measurements of TER and FD4 permeability across intestinal tissue regions mounted in Ussing chambers in Figure 4B-G - isolated from mice 24 h after i.p. injection of IL-6, IFN-γ, TNF-α or IFN-γ + TNF-α and mounted in Ussing chambers – electrogenic ion transport responses to the $Ca^{2+}$ stimulus, carbachol (300 μM) or the cAMP agonist, forskolin (20 μM) were measured in (**A,D**) cecum, (**B**,**E**) proximal colon, (**C**,**F**) and distal colon (n=4). Ion transport responses expressed as the

change in short-circuit current ($\Delta I_{sc}$) in $\mu A/cm^2$. Data are expressed as mean ± SD. Comparisons between genotypes and within treatment groups were by unpaired Student's t-test.

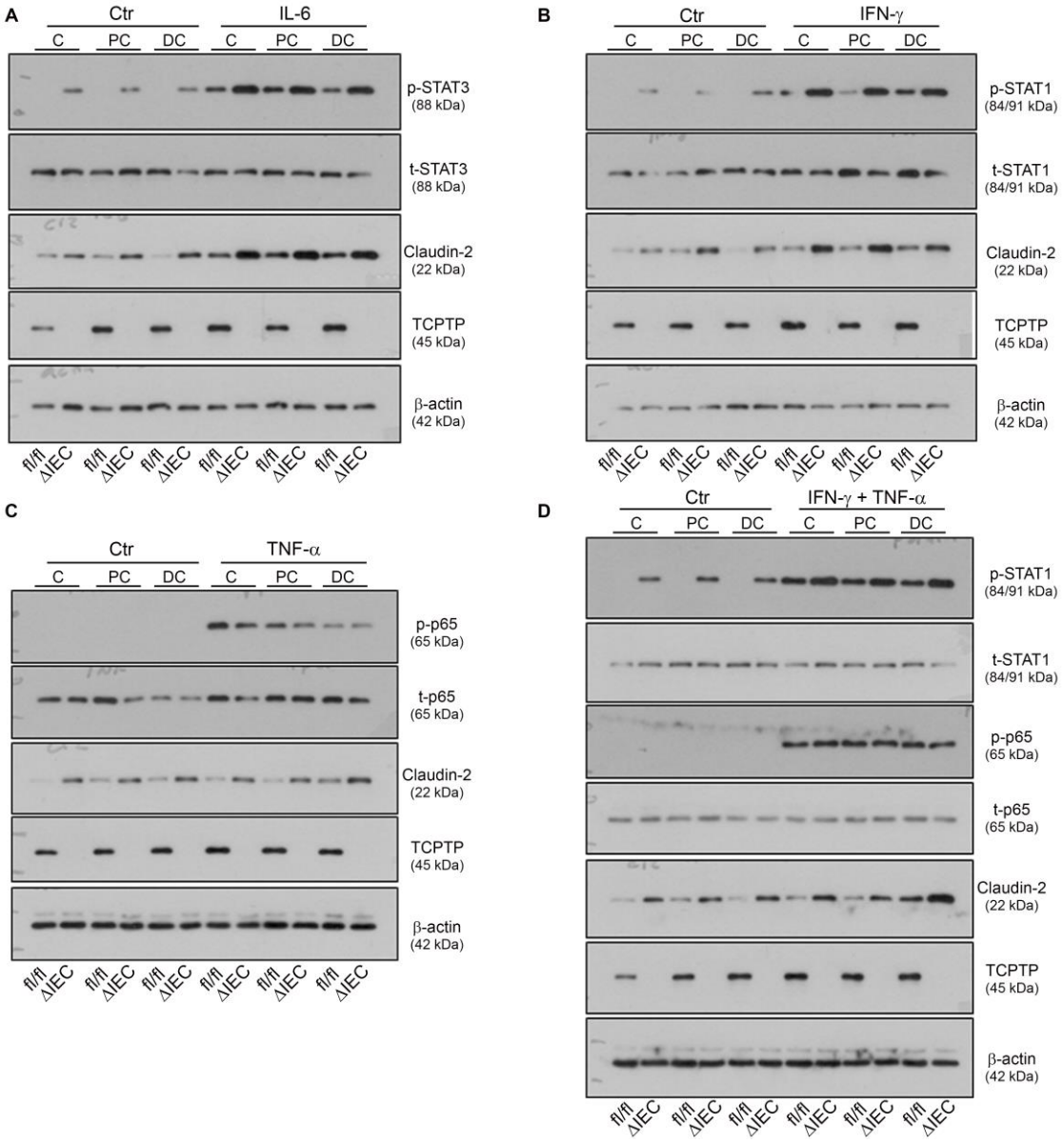


**Supplementary Figure 9. Western blots of claudin-2 and signaling mediators in isolated IECs from cytokine-treated *Ptpn2*$^{\Delta IEC}$knockout mice.** Mice were injected i.p. with (**A**) IL-6, (**B**) IFN-γ, (**C**) TNF-α or (**D**) IFN-γ + TNF-α and tissue collected after 24 h. Epithelial cells from cecum [C], proximal [PC] and distal colon [DC] were isolated from *Ptpn2*$^{\Delta IEC}$ (*ΔIEC*) and *Ptpn2*$^{fl/fl}$ (*fl/fl*) control mice. Cells were lysed and probed by Western blotting for expression of claudin-2 and phosphorylated and total levels of STAT1, STAT3 and NF-κB (p65). Expression of β-actin

was measured as a loading control. Blots are representative of n=4 individual mice per condition.

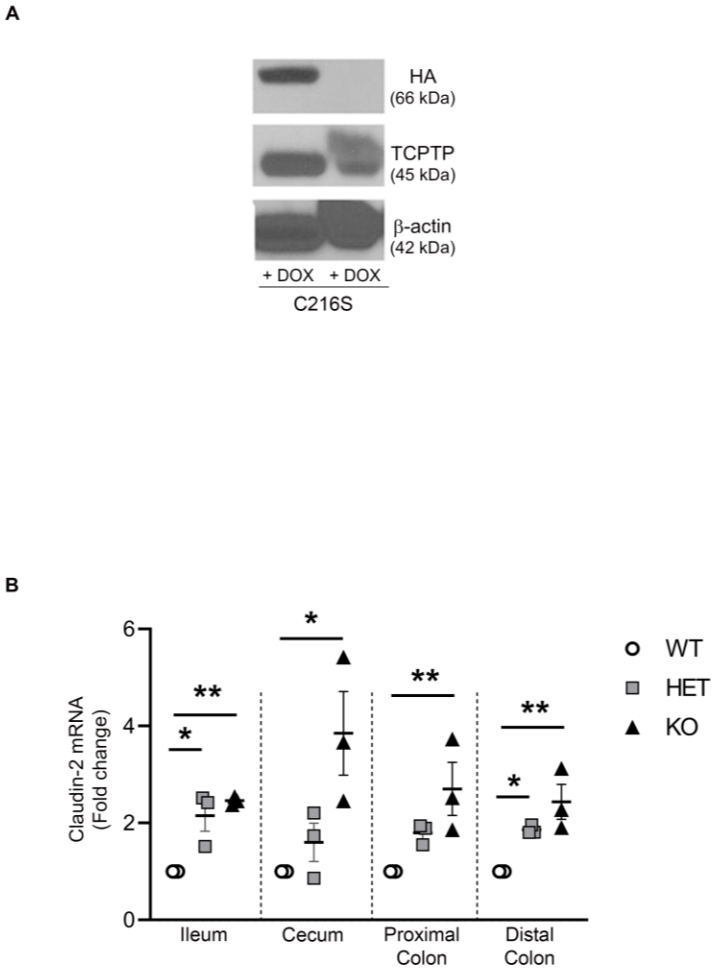


**Supplementary Figure 10. Doxycycline-induced HA-tagged TC45-C216S mutant in transfected HCA-7 intestinal epithelial cells.** (**A**) Western blot showing doxycycline (15 µg/ml; 48 hrs) induced expression of HA-tagged C216S-TC45 in HCA-7 intestinal epithelial cells.

(**B**) Claudin-2 mRNA expression in IECs isolated from intestinal regions (ileum, cecum, proximal and distal colon) of *Tcptp* ET, HET and KO mice normalized to GAPDH (n=3). Data are expressed as mean ± SD. Statistical significance was calculated by 1-way ANOVA and Student-Newman-Keuls post-test. *,P<0.05; **,P<0.01.

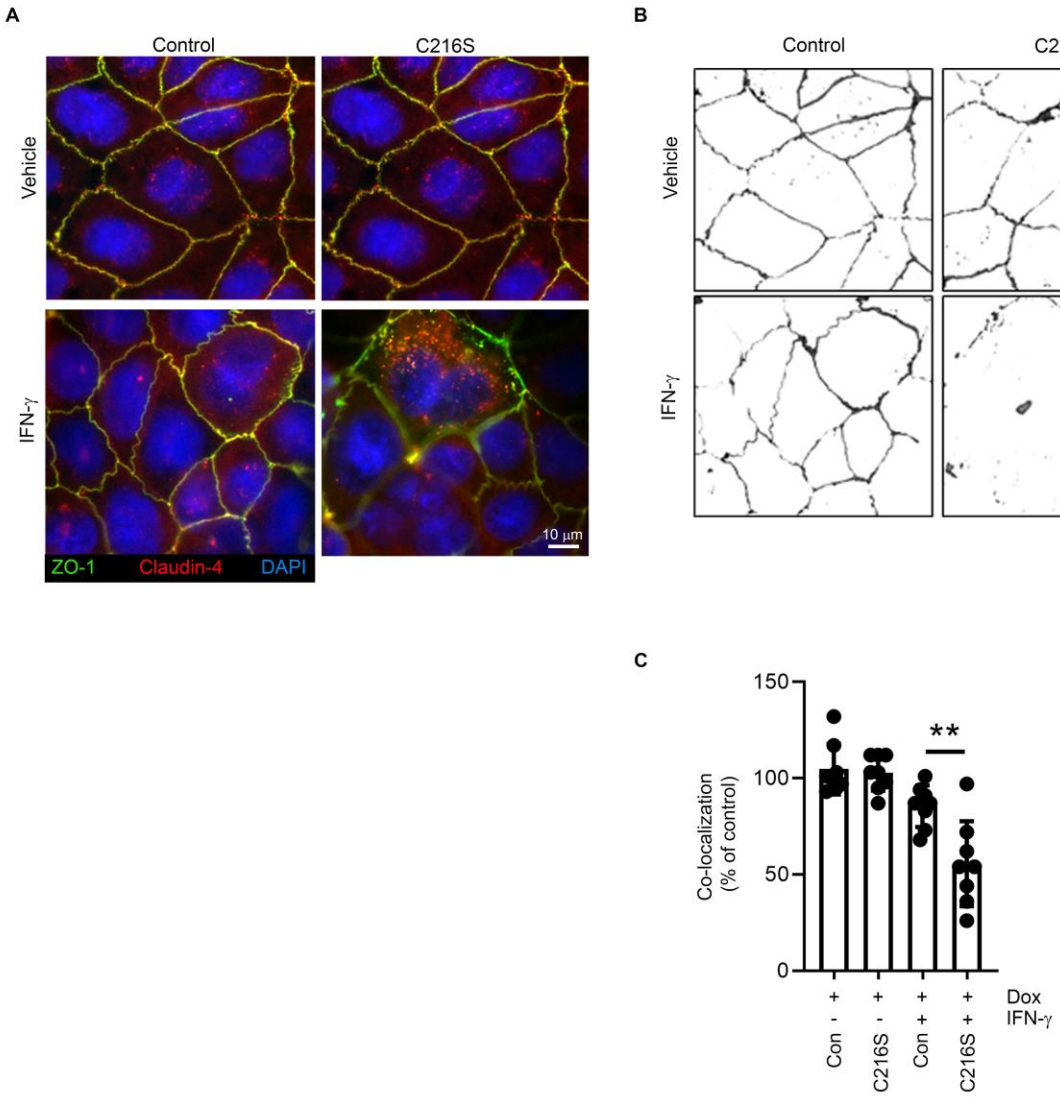


**Supplementary Figure 11. ZO-1/claudin-4 membrane colocalization in IFN-γ treated TC45-C216S HCA-7 IECs.** (**A**) Immunofluorescence images of ZO-1, claudin-4 and nuclear stain (DAPI) following doxycycline (15 μg/ml; 48 hrs) induced expression of HA-tagged C216S-TC45 in HCA-7 intestinal epithelial cells. Following doxycycline treatment, cells were treated with IFN-γ (500 U/mL) or vehicle (PBS) for 24 hrs. (**B**) Line scan imaging showing and (**C**) quantification of ZO-1 and claudin-4 colocalization (n=8). Data are expressed as mean ± SD. Statistical significance was calculated by 1-way ANOVA and Student-Newman-Keuls post-test. **,P<0.01.

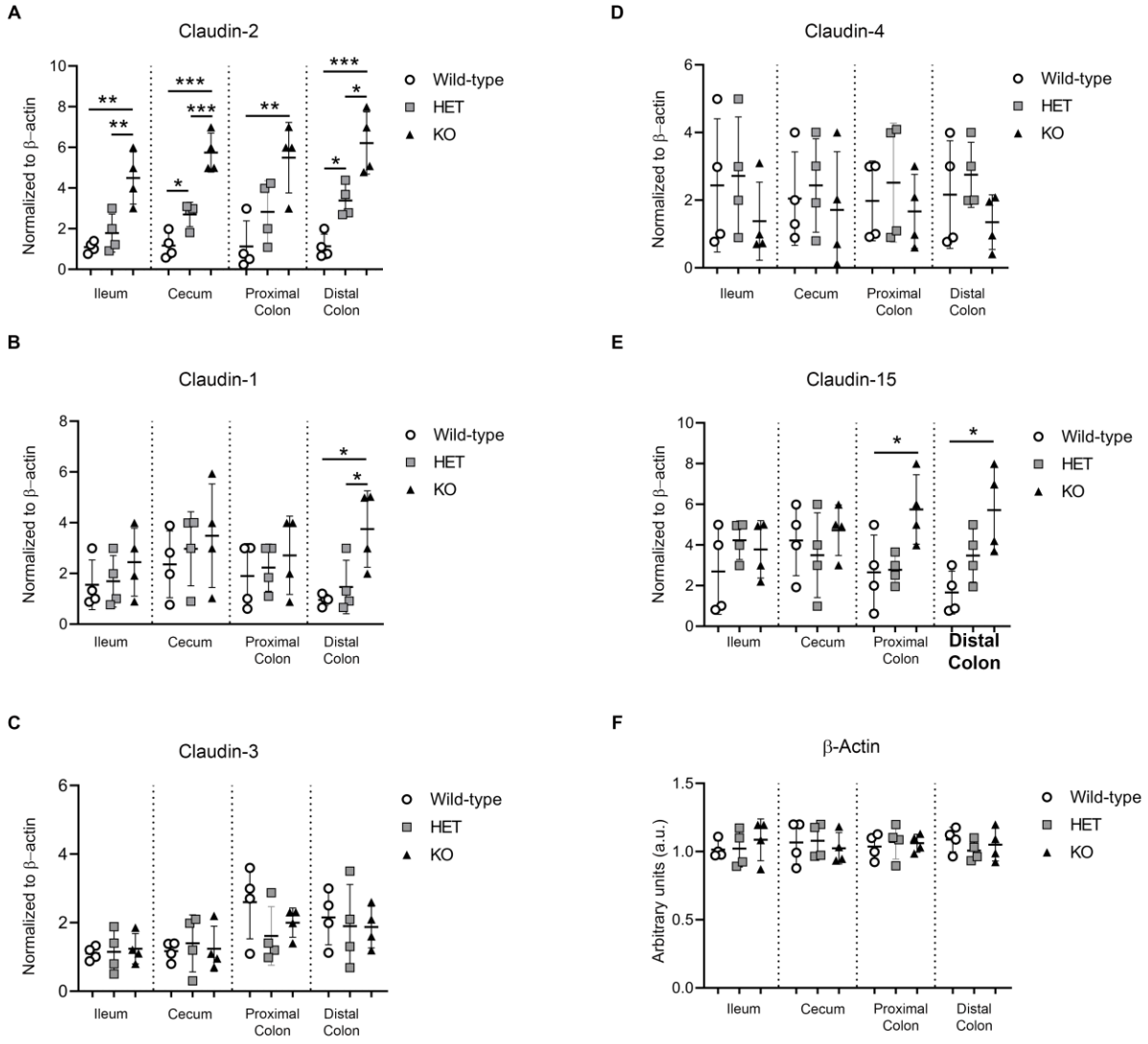


**Supplementary Figure 12. Densitometric analysis of claudin expression in isolated intestinal epithelia cells from intestinal regions of whole-body *Tcptp*-deficient mice.** Western blots of isolated IEC from ileum, cecum, proximal and distal colon of *Tcptp*-WT, *Tcptp*-HET and *Tcptp*-KO mice (shown in Figure 6B), were analyzed by densitometry for quantification of expression of (**A**) claudin-2, (**B**) claudin-1, (**C**) claudin-3, (**D**) claudin-4, (**E**) claudin-15, and (**F**) β-actin (n=4). Data are expressed as mean ± SD. Statistical significance was calculated by 1-way ANOVA and Student-Newman-Keuls post-test. *,P<0.05; **,P<0.01. ***,P<0.001.

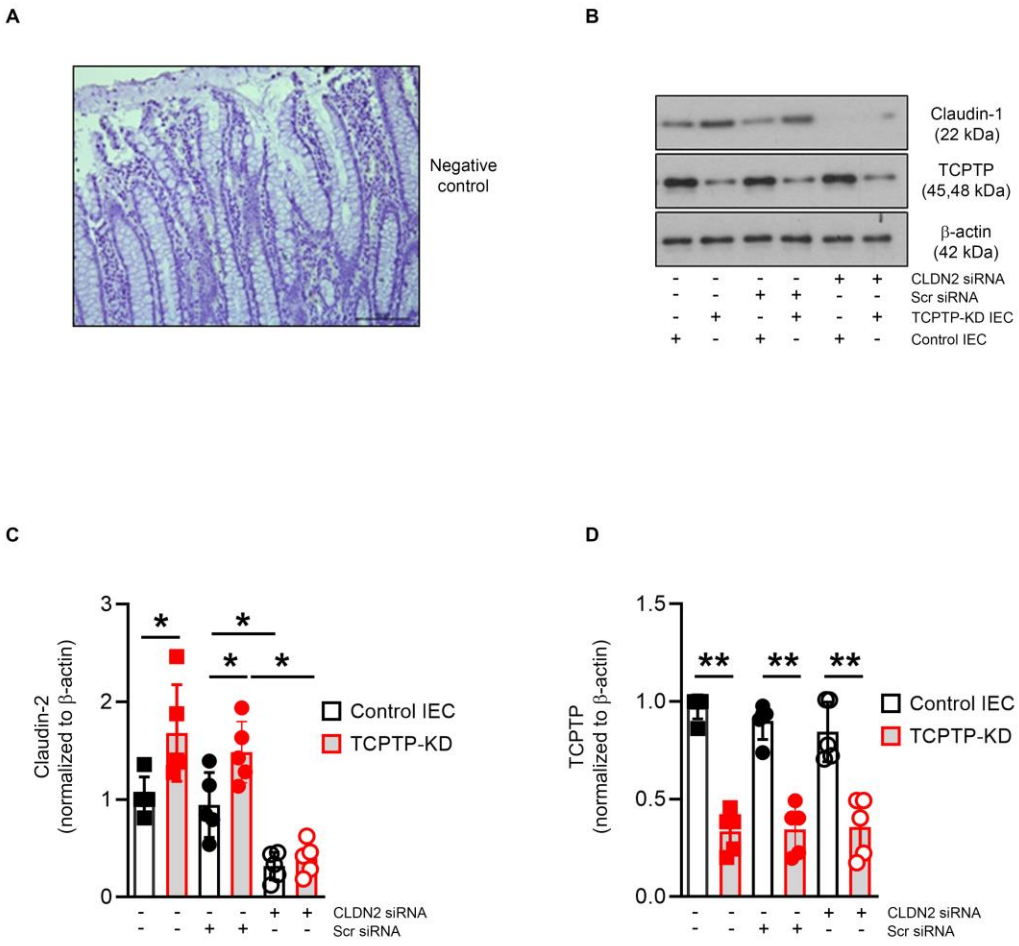


**Supplementary Figure 13. The presence of the *PTPN2* rs1893217 SNP increases ileal claudin-2 expression in IBD.**

(**A**) Negative control for secondary antibody – human colon.

(**B**) Western blots and (**C**) densitometric analysis confirming knockdown of claudin-2 protein in claudin-2 (Cl2) siRNA vs. scrambled (Scr) siRNA transfected control-shRNA and of (**D**) TCPTP in TCPTP-KD Caco-2BBe monolayers. Data are expressed as mean ± SD. Statistical significance was calculated by 1-way ANOVA and Student-Newman-Keuls post-test. *,P<0.05.

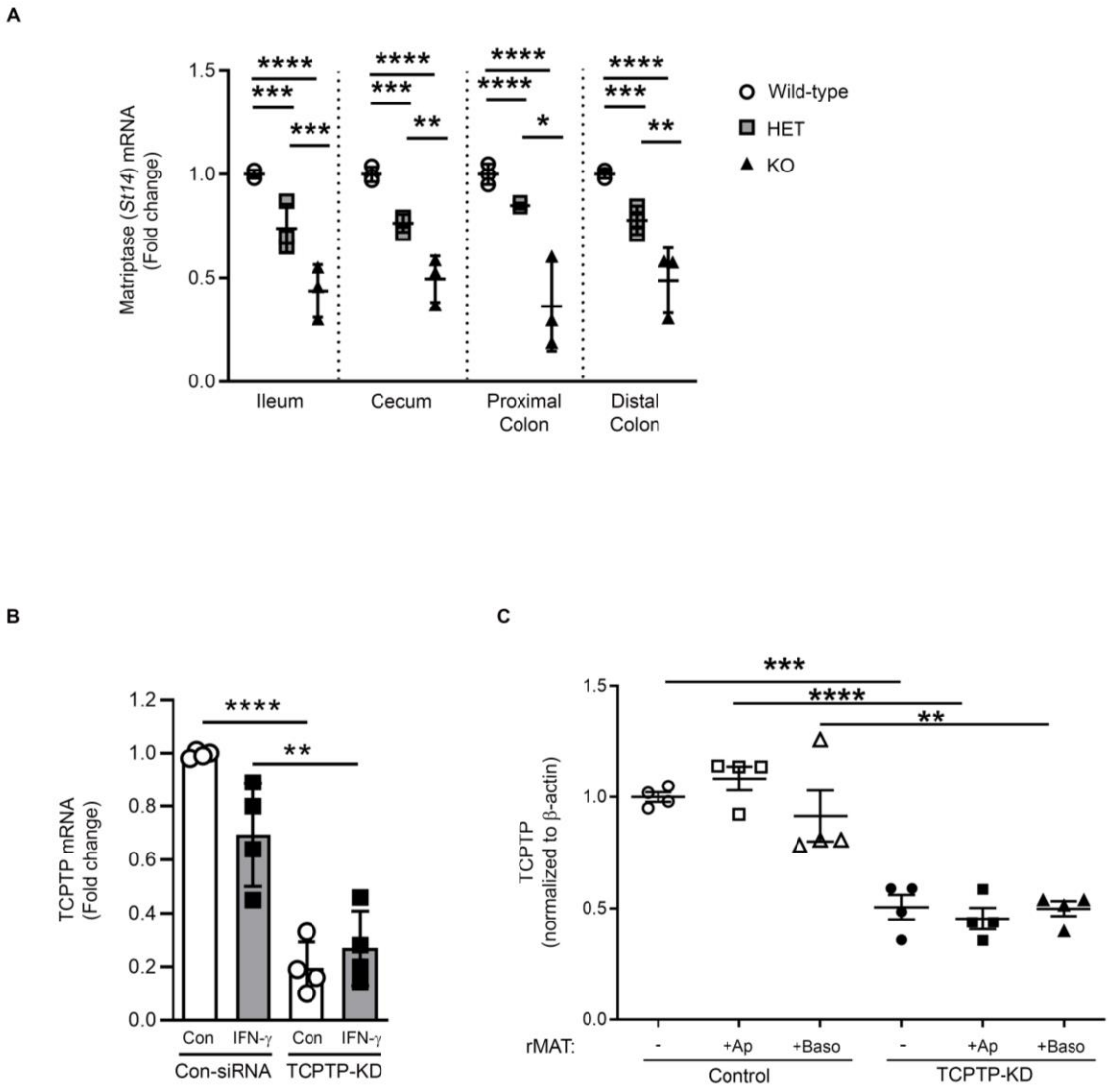


**Supplementary Figure 14. *St14* expression in mouse IECs, and TCPTP mRNA and protein in control and TCPTP-knockdown cells used to study matriptase expression and responses**

(**A**) Matriptase gene expression in IECs isolated from intestinal regions (ileum, cecum, proximal and distal colon) of *Tcptp*-Wild-type, HET and KO mice normalized to GAPDH (n=4). Data expressed as fold change from matriptase levels in *Ptpn2*-Wild-type IECs in each intestinal region.

(**B**) QPCR of *PTPN2* (TCPTP) mRNA levels in control and TCPTP-KD HT-29 IEC used to probe for matriptase (MAT) expression (Fig 7E), confirming siRNA knockdown of TCPTP.

(**C**) TCPTP protein expression in HT-29 cells (control-shRNA and TCPTP-KD) treated with rMAT (Fig 7F,G) was determined by Western blotting and densitometry (normalized to β-actin). Data are expressed as mean ± SD. Statistical significance was calculated by 1-way ANOVA and Student-Newman-Keuls post-test. *,P<0.05, **,P<0.01, ***,P<0.001 and ****,P<0.0001.

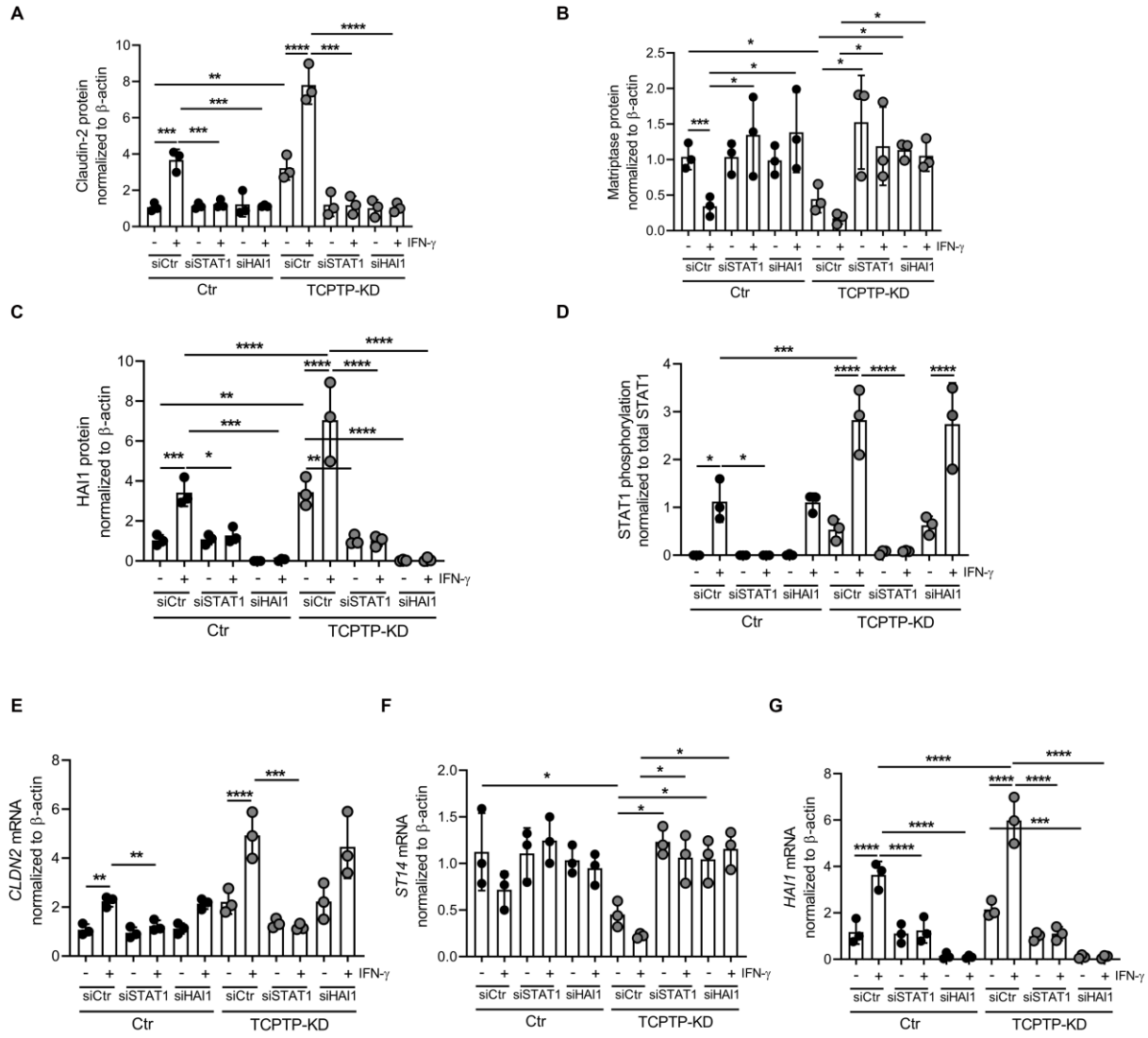


**Supplementary Figure 15. Densitometric analysis of claudin-2 and matriptase protein and gene expression following STAT1 or HAI-1 siRNA knockdown in TCPTP-KD Caco-2 IECs.**

Control-shRNA and TCPTP-KD Caco-2 IECs transfected with control/scrambled siRNA (siCtr), or siRNA targeting STAT1 or HAI1, were probed by Western blot for (**A**) claudin-2, (**B**) matriptase, (**C**) HAI-1, (**D**) phosphorylated (Y701) relative to total STAT1, and normalized β-actin protein levels. (**E**) *CLDN2*, (**F**) *ST14* and (**G**) *HAI1* mRNA levels were determined and normalized to β-actin (n=3). Data are expressed as mean ± SD. Statistical significance was

calculated by 1-way ANOVA and Student-Newman-Keuls post-test. *,P<0.05, **,P<0.01, ***,P<0.001 and ****,P<0.0001.

**Supplementary Table 1: PCR primers**

| Symbol | Species | Primer | Sequence (5´-3´) |
|---|---|---|---|
| PTPN2 | Mouse | Sense | GGTGAAACCAGAACCATATCTC |
| | | Antisense | TTCCATCAGAACAAGACAGG |
| IL13 | Mouse | Sense | GTGCATTTGGCATAACCTGAGC |
| | | Antisense | TCCAGGCTGCTGTACCAATAG |
| St14 | Mouse | Sense | GGGTCCCTACCACAAGAAGTC |
| | | Antisense | GGCAATGTTACAACTCGCTCC |
| CLDN2 | Mouse | Sense | GACAGAGTGGCTGTAGTGGGTG |
| | | Antisense | TGAGATGATGCCCAAGTACA |
| GAPDH | Mouse | Sense | GTTTGTGATGGGTGTGAACCACG |
| | | Antisense | GTGGCAGTGATGGCATGG |
| ACTG2 | Mouse | Sense | GGGTGTGATGGTGGGAATGG |
| | | Antisense | GGTGCTCTTCTGGTGCTACTC |
| PTPN2 | Human | Sense | CAGCCGCTGTACTTGGAAATTCG |
| | | Antisense | ATGTGTTAGGAAGTGGACCCTGTG |
| GAPDH | Human | Sense | AGATCCCTCCAAAATCAAGTGG |
| | | Antisense | GGCAGAGATGATGACCCTTTT |
| CLDN2 | Human | Sense | GCATGAGATGCACAGTCTTC |
| | | Antisense | AGGATCCCATGAAGATTCCAGG |
| ST14 | Human | Sense | CAGCAACAGCAACAAGATCAC |

| | | | |
|---|---|---|---|
| | | Antisense | TGGAGTCGTAGGAGAGGTATTC |
| HAI-1 | Human | Sense | |
| | | Antisense | |
| BamH1 | | Sense | CCTGGAGAAGGATCCATGTACCCAGATGTT |
| M1ul | | Antisense | TAATTCACGCGTGGTACCGTGGACTGCAGAATT |
| Lenti-X-HA vector Forward | | Sense | AGCAGAGCTCGTTTAGTGAACCGT |
| Lenti-X-HA vector Reverse (PS4 R) | | Antisense | TCTCTTGGTCATCTGTTGGCC |
| Tet-on | | Sense | ACAGAGTTCTTGAAGTGGTGGCCT |
| | | Antisense | TGGTTTGTTTGCCGGATCAAGAGC |